Measuring Receiver Diversity on a Low-Altitude UAV in a Ground-to-Air Wireless Mesh Network

H. T. Kung, Chit-Kwan Lin, Tsung-Han Lin, Stephen J. Tarsa, Dario Vlah

Harvard University
Cambridge, MA

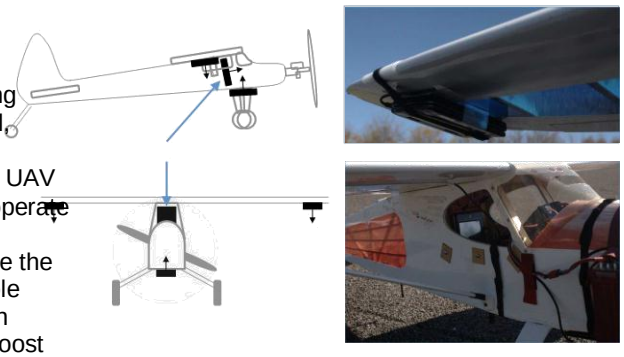

Abstract—We consider the problem of mitigating a highly varying wireless channel between a ground node transmitting to a small, low-altitude unmanned aerial vehicle (UAV) in a wireless mesh network. One approach is to use multiple receiver nodes on the UAV that exploit the channel's spatial/temporal diversity and that cooperate to improve overall packet reception. We present a series of measurement studies from a real-world testbed that characterize the wireless channel between a transmitter ground node and multiple receiver nodes on a UAV. We show that the correlation between receiver nodes is poor and that using four receiver nodes can boost packet delivery rates by some 25%.

I. Introduction

A potentially important use for small, low-altitude unmanned aerial vehicles (UAVs) is providing ad-hoc, ondemand wireless network infrastructure. This capability is generally useful to civilian applications, especially where nodes or users on the ground cannot communicate due to obstructions to line-of-sight, e.g., in emergency natural disaster operations, traffic monitoring and law enforcement surveillance. Commercial-off-the-shelf technologies such as IEEE 802.11 wireless LAN now make it practical to deploy such wireless mesh networks with aerial nodes [1], [2], [3].

However, a key challenge to deployment is achieving good ground-to-air communications. Rapid changes in link quality due to UAV banking maneuvers and outages dictated by environmental shadowing or flight paths translate into a highly varying and lossy wireless channel between ground transmitters and UAV receivers. This is of particular concern to fixed-wing aircraft, which are attractive due to their large cargo capacities, but have physical flight path constraints.

While one approach could be to use better or more powerful radios, the same issues of high link loss and variation would simply arise at larger distances. Since it is well-known that node position and orientation can greatly impact wireless link quality [4], [5], we consider an alternative approach where multiple receiver nodes on-board a UAV cooperate to boost packet delivery rates from a ground transmitter by exploiting the spatial and temporal diversity of the wireless channel.

We present a series of measurement studies on a real-world UAV testbed to (1) characterize the wireless channel between a ground transmitter and multiple UAV receiver nodes and (2) determine the gain achievable by cooperating receivers. Our data show that UAV receiver nodes exhibit poor packet reception correlation over our flight path, especially at short

Fig. 1: Mounting positions of MID nodes on the UAV; arrows show the direction in which the screen of each device faced. The photos show the MID mounted on the starboard wing and inside the cockpit.

time scales. Further, we demonstrate that multiple receivers can be used to improve packet delivery rates significantly.

II. Field Experiment Setup

We collected ground-to-air packet traces by recording individual packet transmissions and receptions between a fixed ground transmitter node and four UAV-mounted receiver nodes. A similar approach can be applied in the air-to-ground direction, and will be addressed in the future. In this section, we describe our experimental setup for collecting these traces.

The UAV we used has a 110” wingspan, a radio-transparent fuselage, and aluminum landing gear and wing struts. Its electric engine is powered by batteries that permit a maximum flight time of 20 minutes. The UAV also has an autopilot that follows a flight path defined by way points. With low wind, it achieves high positional accuracy across laps—e.g., we have found positional deviation with respect to a fixed way point to be no more than 13m when the plane was level, and no more than 25m when the plane was banking through a turn. This permits repeatable data collection over multiple laps within a flight and over multiple flights. During a flight, we log altitude, airspeed, GPS latitude/longitude, and GPS time every 250ms.
At an altitude of 75m, our UAV followed a cyclical, dumbbell-shaped flight path that passed beyond MID radio range at the extremes (Figures 3a–3d). Each lap runs clockwise and, at an airspeed of 20m/s, lasts ~90s. Cruising time for each flight is ~15 minutes, meaning the UAV covers ten laps per flight. We collected packet traces over four flights in total.

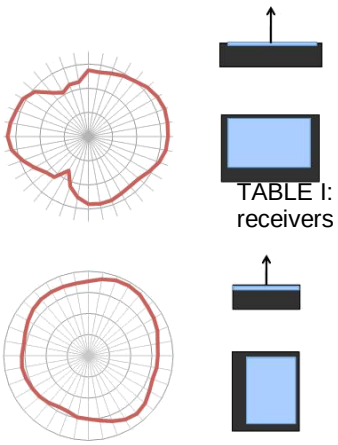

Flight # Rx1 Rx2 Rx3 Rx4 1 0.41
0.44 0.20 0.35
2 0.34 0.37 0.23 0.32 3 0.30 0.38
0.17 0.28 4 0.35 0.40 0.24 0.27

TABLE I: Overall packet delivery rates achieved by the four receivers during four separate flights.

Flight # Full Loss Intermediate No Loss 1
47.3% 18.6% 34.1%
2 54.8% 18.3% 26.9% 3 55.1% 16.1%
28.8% 4 52.5% 18.3% 29.2%

Fig. 2: RSS in dB where the MID receiver is rotated about one axis, as measured in an anechoic chamber. Upper: 180–360◦ give the RSS that the cockpit-mounted receiver experiences as it passes over a fixed ground transmitter; Lower: 0–180◦ give the RSS that the wing-mounted receivers experience; similarly, 180–360◦, for the undercarriage-mounted MID.

These flights were conducted at a property surrounded by woods and farmland, free of 802.11 radio traffic.

Our wireless mesh network nodes were Mobile Internet Devices (MIDs) that feature an 800MHz x86-compatible Intel Atom processor, a Marvell SD8686 802.11b/g internal SDIO radio, an internal omnidirectional antenna and Ubuntu Linux 8.04. One transmitter MID was placed amid tall grass and brush, elevated 20cm from the ground, with its screen facing skyward. Its location is shown as a square in Figures 3 and 4. Four receiver MID nodes (Rx1 to Rx4) were mounted on the UAV as shown in Figure 1. Rx1 and Rx2 were mounted with screens facing the ground, one on the underside of each wing tip. Rx3, with its screen facing skyward, was mounted between the landing gear and Rx4, with its screen facing the bow, was mounted inside the cockpit. The direction of mounting is significant since measurements we took in an anechoic chamber demonstrate that the MID's antenna pattern is asymmetric (Figure 2). Thus, our mounting configuration provides diversity in antenna patterns and offers different shadowing profiles from the landing gear, engine and batteries.

We placed all the nodes in ad-hoc mode at the 1Mbps modulation. We use this modulation to achieve better radio range and because our trace collection tool uses 802.11 broadcast packets (as opposed to unicast packets, which can use other modulations with higher bitrates). To collect traces, our transmitter broadcasts 1420-byte UDP packets, with unique sequence numbers, at 80 pkt/s. The receiver nodes on the UAV run a client that logs the sequence number and timestamp of each received packet.

III. Experiment Results

In this section we present experiment results and discuss their significance. We begin with a look at basic properties of

TABLE II: Percent of flight traces with full loss, intermediate signal, and no loss, determined using a 20-packet window.

the collected data. Next, we examine the gain obtained with more than one receiver. Lastly, we discuss various sources of diversity gain and evaluate their contribution.

A. Single-link Performance To gain a high-level understanding of reception behavior we

analyzed our collected traces as follows. For each receiver, we first divide its packet traces into 20-packet windows, forming a windowed trace for each flight, and then calculate the packet loss rate over each window. This window size captures the loss rate over a reasonably short distance: 20 packets corresponds to 250ms of flight time, or roughly 5m at a nominal airspeed of 20m/s. Figures 3a–3d plot the location of each window from all four flights and categorize each window as no loss (green; 0% loss), full loss (red; 100% loss) or intermediate loss (yellow; all others). Table I contains the overall packet delivery rates for each receiver and each flight.

At first glance the overall packet loss rates seem quite high. However, it is useful to separate the regions where the UAV is out of range, since those regions could make the loss rates seem arbitrarily high. Hence, Table II shows the makeup of each flight out of the different loss categories. We can see that after factoring out the full loss portions, the traces consist of significant amounts of both the no loss and intermediate loss regions. We point out two major implications of these findings. First, the periodic full- and intermediate-loss regions will be an important factor in UAV network protocol design, especially with use of legacy protocols such as TCP which are sensitive to packet loss patterns. Secondly, the large presence of intermediate loss regions indicates that we could obtain significant gains through the use of receiver diversity, given that the losses at different receivers are not correlated. We explore this possibility in the next section.

B. Diversity Results Figures 3a–3d show that the loss regions are different in size
and location across the four receivers. This is further confirmed

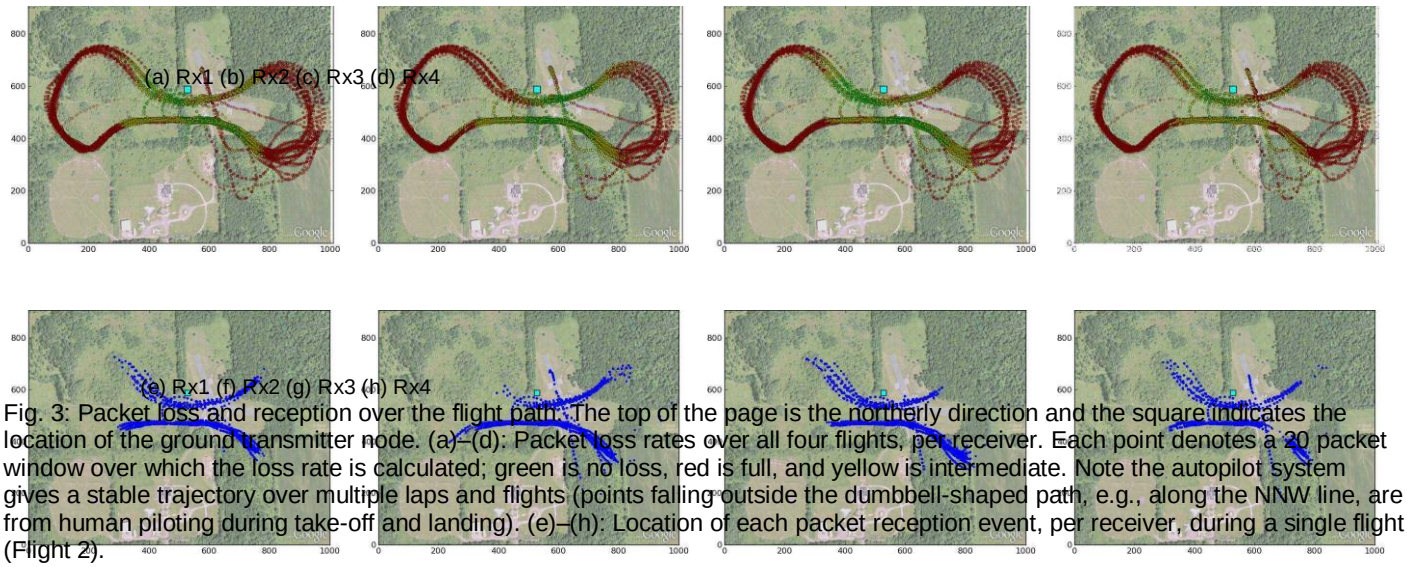

(a) Rx1 (b) Rx2 (c) Rx3 (d) Rx4

(e) Rx1 (f) Rx2 (g) Rx3 (h) Rx4

Fig. 3: Packet loss and reception over the flight path. The top of the page is the northerly direction and the square indicates the location of the ground transmitter node. (a)–(d): Packet loss rates over all four flights, per receiver. Each point denotes a 20 packet window over which the loss rate is calculated; green is no loss, red is full, and yellow is intermediate. Note the autopilot system gives a stable trajectory over multiple laps and flights (points falling outside the dumbbell-shaped path, e.g., along the NNW line, are from human piloting during take-off and landing). (e)–(h): Location of each packet reception event, per receiver, during a single flight (Flight 2).

in Figures 3e–3h, which takes a packet trace from a single representative flight (Flight 2) and simply plots the location of each received packet over the course of the flight for each receiver node. For instance, Rx1 receives packets in the NW quadrant (i.e., on approach towards the ground node), but Rx2 does not until it is almost flying over the ground node.

The above behaviors led us to examine the reception correlation amongst pairs of nodes over the course of a flight (Flight 2). To do so, we first synchronize the packet traces of two receiver nodes, generate the windowed traces for each as before, and then calculate the correlation coefficient ρof the packet reception pattern in pairs of windows corresponding to the same location along the flight path. Note that the correlation coefficient is not defined for any window pair in which at least one window has either no loss or full loss; we ignore such window pairs as a result. We performed this operation for all pairs of receivers.

Figure 4 plots the results for each receiver pair. The color of each data point represents the ρ value for that location. Receivers mounted externally (Rx1, Rx2, and Rx3) were wellcorrelated when the UAV passed close to the ground node, but were poorly correlated further away. This is also demonstrated in Figure 5, which is a normalized histogram of the ρvalues from Flight 2 for each receiver pair. While all pairs have significant mass in ρ=[-0.2,0.2], indicating a general lack of correlation over most of the flight path, only externallymounted node pairs show an additional large peak at ρ=1.0, a region of high correlation where the UAV passes near the ground node. In contrast, pairs (Rx1, Rx4) and (Rx2, Rx4), which correspond to the wing/cockpit node pairs, lack this peak entirely and are actually the most uncorrelated nodes since they have the overall largest peaks at ρ = 0.1. This disparity is due to Rx4 being mounted in the cockpit and having an antenna orientation significantly different from that of the wing-mounted nodes (see Figure 2). Taken together, these results indicate that receivers are uncorrelated over large portions of the flight path and suggest that employing multiple nodes to cooperatively boost receiver diversity can help improve packet delivery rates on-board the UAV.

To determine the gain due to receiver diversity, we combine the packet receptions at the four receivers into a combined trace, where a packet is marked as received if it was received by at least one individual receiver. Table III shows the overall delivery rates of combined traces for each flight, alongside the best single receiver's delivery rate. We can see that diversity brings about an additional gain of roughly 25%.

C. Diversity over time We next discuss the availability of diversity gain at various
time scales in our experiments. First, on large time scales of, say, one flight lap, the reception traces are clearly correlated, resulting from all nodes experiencing nearly identical path loss. As the mobile node moves far enough out of range of the transmitter, the loss of signal strength due to distance cannot be overcome by small differences between the receivers. Thus, receiver diversity might not help much here since all receivers undergo the same outage. Similarly, when the receivers are in close proximity of the transmitter, the loss rate is low enough that diversity cannot significantly improve it.

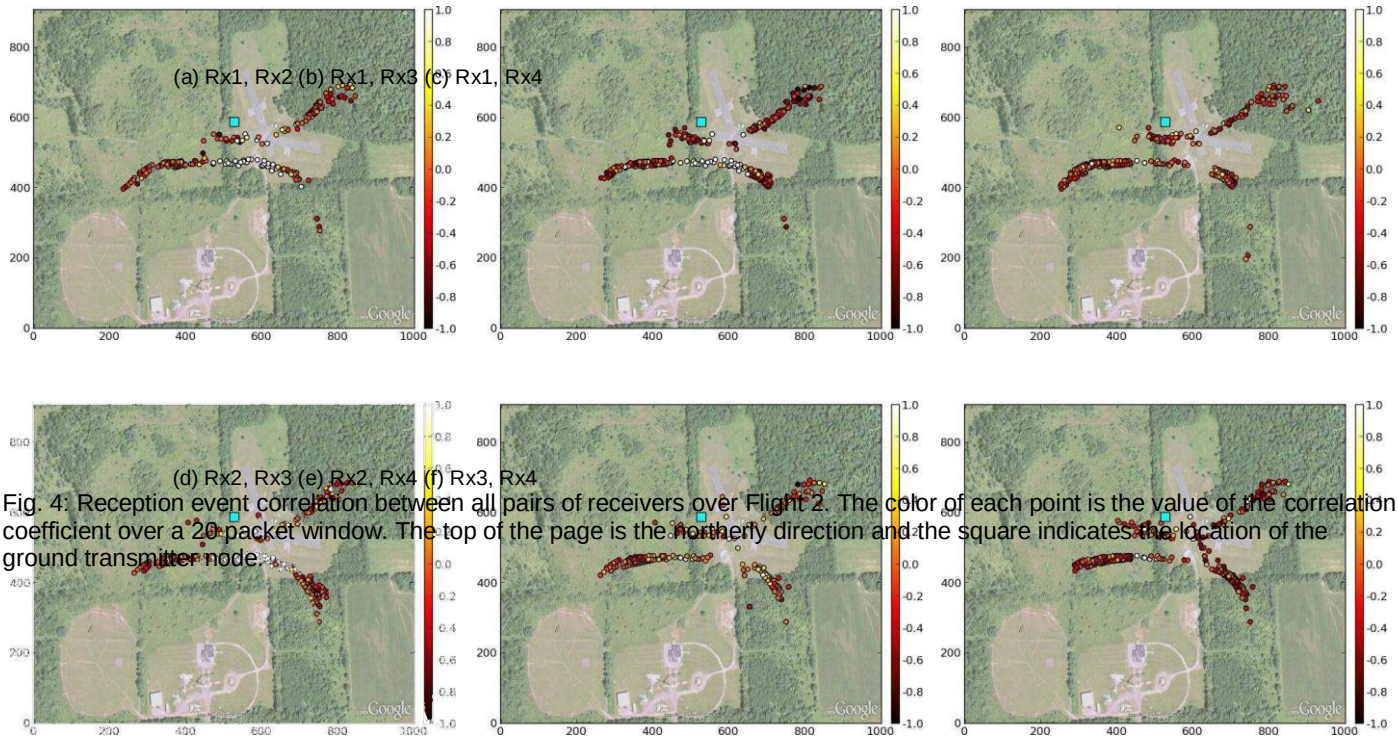

(a) Rx1, Rx2 (b) Rx1, Rx3 (c) Rx1, Rx4

(d) Rx2, Rx3 (e) Rx2, Rx4 (f) Rx3, Rx4

Fig. 4: Reception event correlation between all pairs of receivers over Flight 2. The color of each point is the value of the correlation coefficient over a 20-packet window. The top of the page is the northerly direction and the square indicates the location of the ground transmitter node.

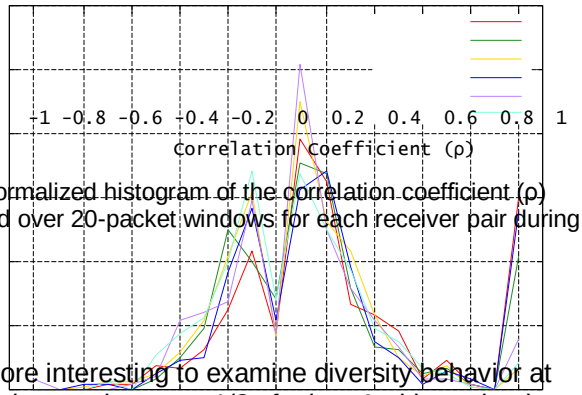

Fig. 5: Normalized histogram of the correlation coefficient (ρ) calculated over 20-packet windows for each receiver pair during Flight 2.

It is more interesting to examine diversity behavior at medium time scales, e.g., 1/8 of a lap. At this scale, the distance may not change enough to cause a major shift in path loss, and thus other effects become more pronounced. Namely, links may be shadowed diversely by various obstructions, such as the airplane as it banks, or even external objects like trees.

Lastly, on small time scales, where path loss does not change significantly due to either changing distance or shadowing, links may still undergo independent rapid variations due to fast fading. Fast fading occurs when multipath signals combine with a varying phase difference, e.g. due to Doppler effect or varying path lengths. The salient question is whether fast fading is present in our experiment environment, and if so, to what extent it occurs independently at each receiver.

We evaluate diversity at different time scales in two ways. First, we compute the correlation of all receiver pairs over increasing time spans. Secondly, we compare the diversity gain in our traces to that of synthetic traces generated using a Bernoulli process.

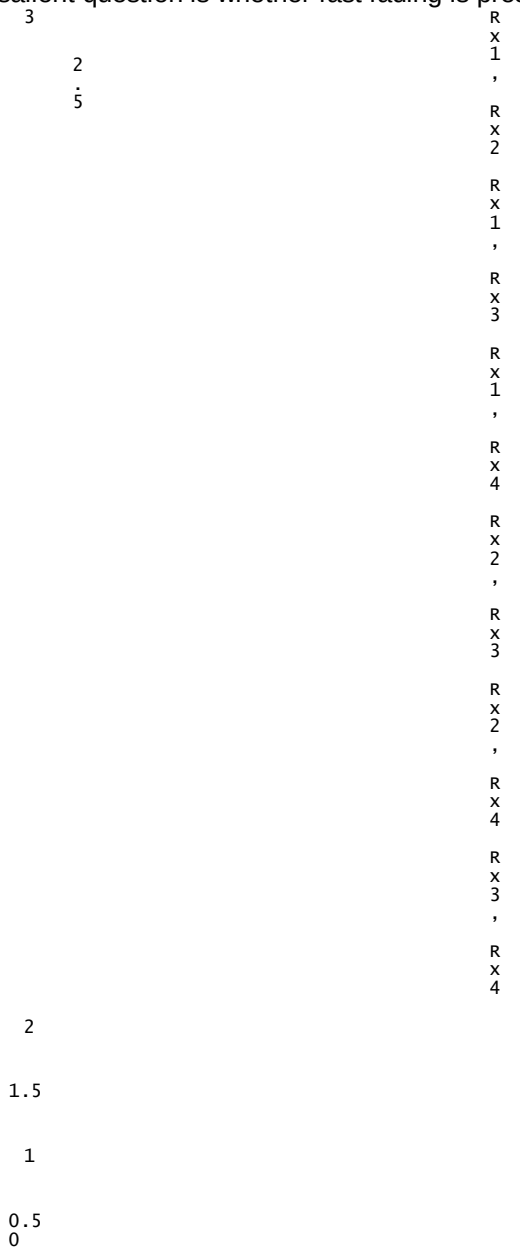

	Flight 1	Flight 2	Flight 3	Flight 4
Best single receiver Rx2 Rx2 Rx2 Rx2				
	0.55	0.49	0.46	0.51
	25%	32%	21%	28%
Best single delivery rate	0.44	0.37	0.38	0.40
Combined delivery rate				
Percent improvement				

TABLE III: Overall packet delivery rates achieved by the four receivers during four separate flights.

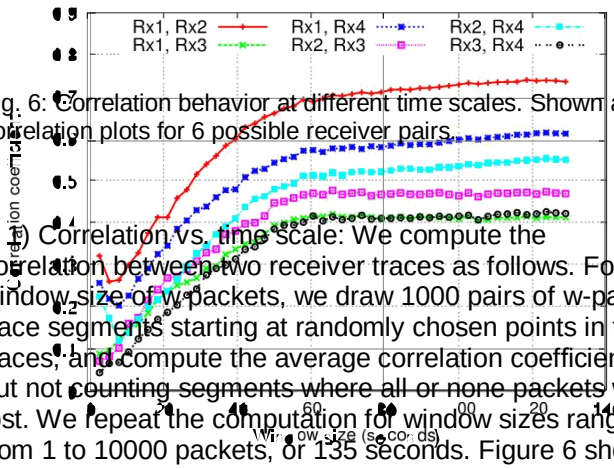

Fig. 6: Correlation behavior at different time scales. Shown are correlation plots for 6 possible receiver pairs.

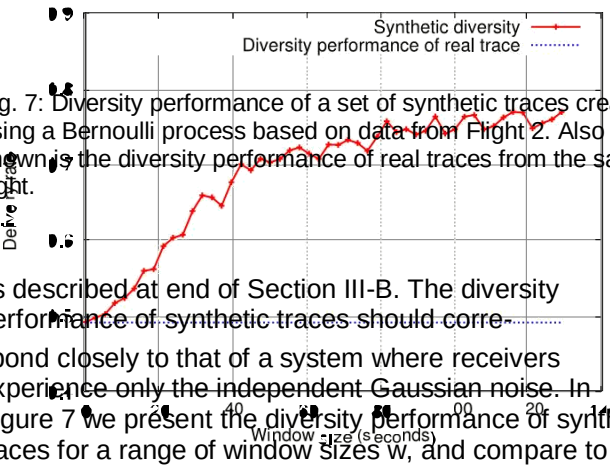

Fig. 7: Diversity performance of a set of synthetic traces created using a Bernoulli process based on data from Flight 2. Also shown is the diversity performance of real traces from the same flight.

2) Correlation vs. time scale: We compute the correlation between two receiver traces as follows. For a window size of w packets, we draw 1000 pairs of w-packet trace segments starting at randomly chosen points in the traces, and compute the average correlation coefficient, but not counting segments where all or none packets were lost. We repeat the computation for window sizes ranging from 1 to 10000 packets, or 135 seconds. Figure 6 shows the resulting correlations.

Two features stand out in the plot. First, there is a clear difference between the correlation of different receiver pairs. The pair with most correlation, Rx1 and Rx2, are the two receivers mounted on the underside of the wings, corroborating the finding from Section III-B. At the same time, the pair with least correlation seems to be Rx3 and Rx4, which differ not only in mounting orientation but also in the nature of line-ofsight obstruction; Rx3 is mounted on the UAV's bottom while Rx4 is inside the cockpit area.

The second main feature of the plot is the apparent sharp increase in correlation at window sizes of up to about 60s. This time scale is large enough that it covers both in- and outof-range regions of the flight path, where all receivers start to experience the same large-scale path-loss effects. Below this window size, however, correlation decreases, indicating a lack of dependence due to fading. Finally, as window size decreases further, the correlation increases again due to increasing fraction of windows with all or no packet losses, skewing the average correlation coefficient.

2) Comparison with Bernoulli traces: We now look for further evidence of independent packet loss behavior at short time scales. In particular, we compare the collected traces to synthetic traces constructed as follows. Let us divide a collected trace into N segments of length w packets. For each segment, we compute the mean packet delivery rate, p_{ii}. For each p_i, we construct a synthetic packet loss sequence by performing w Bernoulli trials with parameter p. Finally, we concatenate the N segments, repeat the process for all receivers' traces, and merge the traces into a combined trace as described at end of Section III-B. The diversity performance of synthetic traces should correspond closely to that of a system where receivers experience only the independent Gaussian noise. In Figure 7 we present the diversity performance of synthetic traces for a range of window sizes w, and compare to performance of the system in our experiment. We can see that, indeed, the performances match very closely at short time scales, and begin to diverge at window sizes similar to those of increasing correlation in Figure 6. This seems to indicate that fading has little effect in our environment, and that packet loss behavior is largely independent at short time scales.

IV. Conclusions

In this paper we presented results of an experimental study of ground-to-air UAV links. We found that the links are bursty, owing to the UAV moving in and out of range; this might be a property specific to fixed-wing craft, but is important nonetheless as those are the most efficient class of fliers. As a result, network layer protocols will need to be adapted to be aware of link layer losses, or to work on top of link layer mechanisms which use, e.g., coding or retransmissions to mask the loss.

At small time scales of up to 1000 packets, or about 10 seconds, we found that the packet losses seem to be uncorrelated, giving diversity performance very similar to that of synthetic traces generated using Bernoulli trials. This seems to indicate that the effect of fast fading is not significant in our environment in any direction; that is, fading does not result in either better or worse diversity performance than that of memoryless losses.
The diversity gain we observed with four receiver nodes consisted of a 25% increase in delivery rate over the course of one hour of UAV flight. The salient question is whether this is sufficient to warrant the addition of extra receivers on a UAV; in the event that the extra receivers are already present

due to other application requirements, using them for diversity reception would provide a clear and inexpensive benefit.

ACKNOWLEDGEMENTS

This material is based on research sponsored by Air Force Research Laboratory under agreement numbers FA8750-092-0180 and FA8750-10-2-0180. The U.S. Government is authorized to reproduce and distribute reprints for Governmental purposes notwithstanding any copyright notation thereon. The views and conclusions contained herein are those of the authors and should not be interpreted as necessarily representing the official policies or endorsements, either expressed or implied, of Air Force Research Laboratory or the U.S. Government.

REFERENCES

[1] T. Brown, B. Argrow, C. Dixon, and S. Doshi, “Ad Hoc UAV Ground Network (AUGNet),” in AIAA 3rd “Unmanned Unlimited” Technical Conference, 2004.

[2] A. Ryan, X. Xiao, S. Rathinam, J. Tisdale, M. Zennaro, D. Caveney, R. Sengupta, and J. K. Hedrick, “A modular software infrastructure for distributed control of collaborating uavs,” in Proc. AIAA Conf. on Guidance, Navigation and Control, 2006.

[3] D. Hague, H. T. Kung, and B. W. Suter, “Field experimentation of cotsbased uav networking,” in MILCOM, 2006.

[4] D. Aguayo, J. Bicket, S. Biswas, G. Judd, and R. Morris, “Link-level measurements from an 802.11b mesh network,” in SIGCOMM, 2004.

[5] J. Bicket, D. Aguayo, S. Biswas, and R. Morris, “Architecture and evaluation of an unplanned 802.11b mesh network,” in MobiCom, 2005.